[3] Potter, J L , Kinslow, M , Arney, G D , Jr , and Bailey, A B , "Description and preliminary calibration of a low-density, hypervelocity wind tunnel," Arnold Eng Dev Center AEDC-TN-61-83 (August 1961)

[4] Aroesty, J , ' Pressure distributions on flat plates at Mach 4 and low density flow, ' Univ Calif , TR HE-150-157 (July 28, 1958)

[5] Nagamatsu, H T , Sheer, R E , Jr , and Schmid, J R , "High temperature rarefied hypersonic flow over a flat plate," ARS J 31, 902–910 (1961)

[6] Hayes, W D and Probstein, R F , *Hypersonic Flow Theory* (Academic Press, Inc , New York, 1959), Chap 9

[7] Vidal, R J , Golian, T C , and Bartz, J A "An experimental study of hypersonic low-density viscous effects on a sharp flat-plate," AIAA Preprint 63-435 (August 1963)

[8] Aroesty, J , "Strong interaction with slip boundary condi tions," Aeronaut Res Labs Rept 64 (September 1961)

Velocity Profiles from Compressible Wall Jets

ROBERT LEROY LAWRENCE*
The Boeing Company, Renton, Wash

THE flow over afterbodies downstream from the fan-nozzle annulus of a fanjet engine is axially symmetric wall-jet flow As part of an experimental investigation to predict the drag on such afterbodies, the author has measured total pressure profiles in the flow over a 3-in -diam model, which consisted of a nosepiece, a convergent fan nozzle, a cylindrical afterbody, and a total pressure rake (Fig 1) The freestream air was supplied by an induction tunnel with a 20-in free jet

The flow from the convergent nozzle was compressible; the nozzle pressure ratio $(Pt/P)_f$ was varied from 2 0 to 4 4 The data are reported for $20 < X/h < 133$ and $2 < X/R_1 < 8$ The afterbody surfaces were smooth to 0 0001 in The freestream Mach number M_∞ was 0 and 0 8

Velocity Profiles for $M_\infty = 0$

The velocity U is defined as the fully expanded velocity from the indicated total pressure to the freestream static pressure A constant total temperature, usually equal to the nozzle total temperature, was assumed to exist throughout the mixing region The velocity profiles were nondimensionalized in the usual way: the radial distance from the afterbody surface r is divided by δ_2, which is the value of r at $(U_{max} + U_\infty)/2$; and U is divided by the maximum velocity for the profile, U_{max}

Figures 2 and 3 compare the present compressible data with Glauert's incompressible, two-dimensional profile of

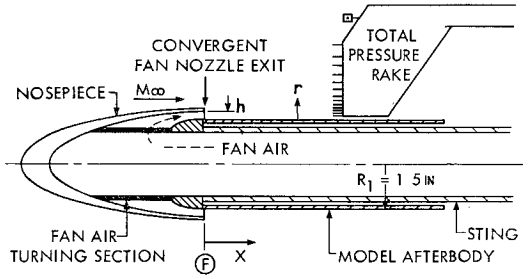

Fig 1 Model to simulate fan-nozzle annulus

Received December 27, 1963
* Research Engineer, Propulsion Staff, Airplane Division

Ref 1 Over the range of geometries and pressure ratios tested, the experimental data closely follow Glauert's profile; it can be concluded that the effects of compressibility and axial symmetry are negligible

Velocity Profiles for $M_\infty = 0\ 8$

The velocity profiles are given in terms of a velocity difference parameter $(U - U_\infty)/(U_{max} - U_\infty)$ It is expected that, when $U_{max} \to U_\infty$, the profiles should be more strongly affected by skin friction; conversely, when $U_{max} \gg U_\infty$, the velocity difference between the fan exit velocity and U_∞ will be large, and the profiles should be strongly affected by mixing

Figure 4 is a case where $U_{max} \gg U_\infty$ Since mixing predominates, the choice of $(U - U_\infty)/(U_{max} - U_\infty)$ for the

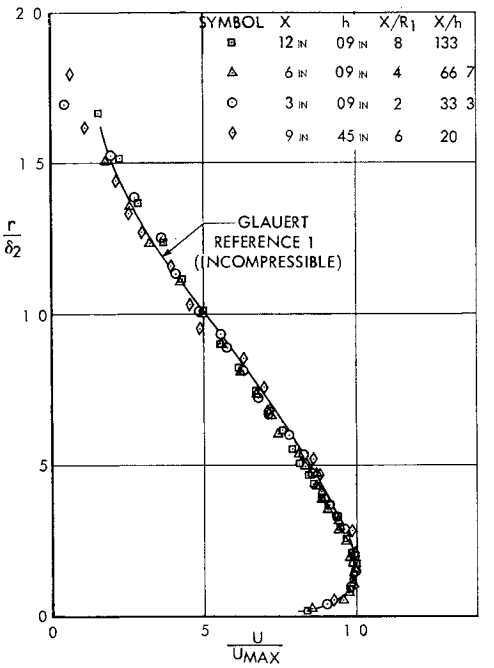

Fig 2 Axisymmetric compressible wall-jet velocity profiles; $M_\infty = 0$, $(Pt/P)_F = 2\ 0$, convergent nozzles

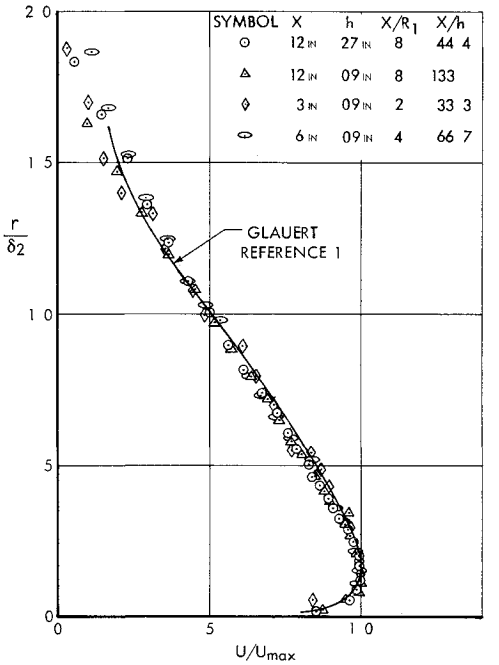

Fig 3 Axisymmetric compressible wall-jet velocity profiles; $M_\infty = 0$, $(Pt/P)_F = 4\ 4$, convergent nozzles

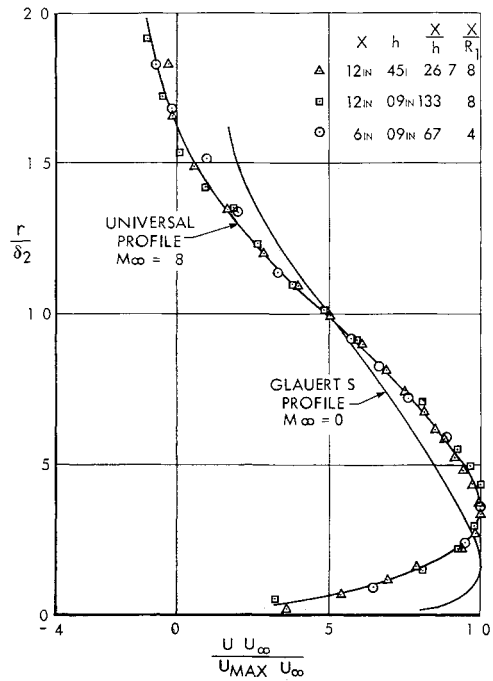

Fig 4 Axisymmetric compressible wall-jet velocity profiles; $M_\infty = 0\,8$, $(Pt/P)_F = 4\,4$, convergent nozzles

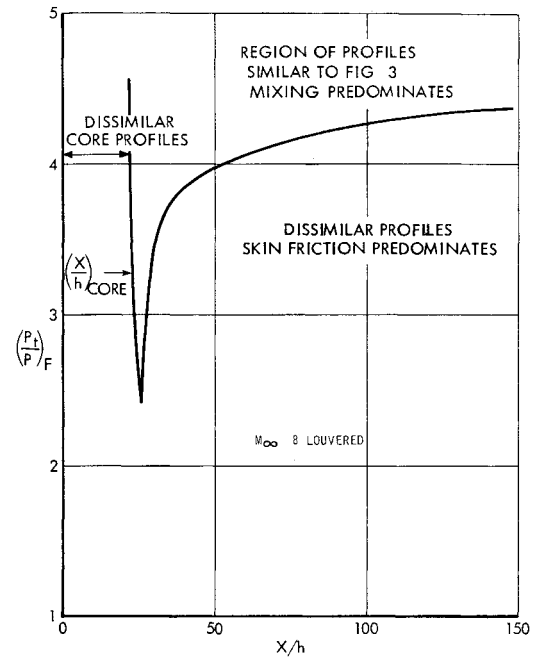

Fig 6 Axisymmetric compressible wall jet: region of profile similarity; $M_\infty = 0\,8$, convergent nozzles

ordinate allows the data to be represented by a single universal profile; Glauert's profile for $M_\infty = 0$ is compared, and it differs considerably

Figure 5 is a case where $U_{max} \rightarrow U_\infty$; here the skin friction predominates, and none of the profiles fall on the universal profile for $M_\infty = 0\,8$ (from Fig 4) Profiles at other values of $(Pt/P)_F$, X/h, and X/R_1 were plotted (not shown) and compared with the profile of Fig 4 Figure 6 was constructed to show the approximate region of applicability of the universal profile of Fig 4 The curve $(X/h)_{\infty\,e}$ vs $(Pt/P)_F$ was estimated from data taken during the experiment; it represents the expected length of the core region

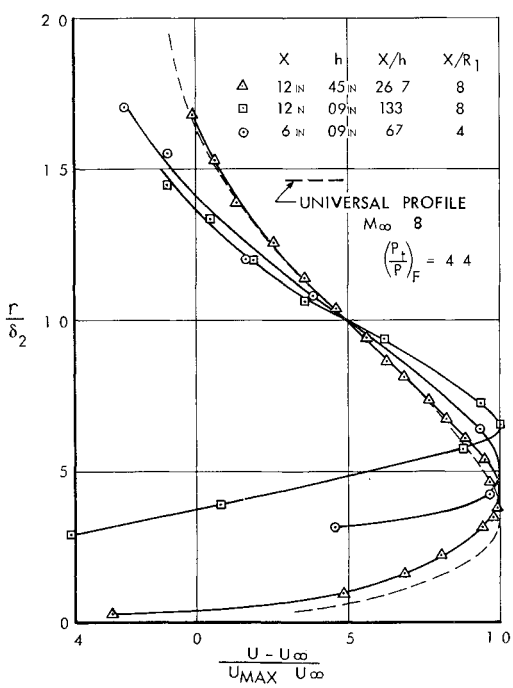

Fig 5 Axisymmetric compressible wall-jet velocity profiles; $M_\infty = 0\,8$, $(Pt/P)_F = 2\,0$, convergent nozzles

Reference

[1] Glauert, M B, "The wall jet," J Fluid Mech 1, 625–643 (1956)

Wave Propagation in Rotating Elastic Media

RONALD L HUSTON*
University of Cincinnati, Cincinnati, Ohio

The effect of "rigid-body" rotation on wave propagation velocities in elastic media is investigated It is found that the rotation generates a coupling between the classical longitudinal and transverse waves The rotation tends to increase the propagation velocity of transverse-type amplitude waves while decreasing the propagation velocity of longitudinal-type amplitude waves For phase waves, which are associated with vibratory motion, the situation is found to be reversed

Introduction

IT is a well-known result that, in an unbounded homogeneous isotropic elastic medium, disturbances are propagated as longitudinal or transverse waves with velocities $[(\lambda + 2\mu)/\rho]^{1/2}$ and $[\mu/\rho]^{1/2}$, respectively, where λ and μ are Lame's elastic constants and ρ is the mass density of the medium The purpose here is to investigate the effect of "rigid body" rotation of the elastic medium on these propagation velocities

Received January 8, 1964 The author is grateful to M A Brull of the University of Pennsylvania for suggesting this investigation

* Assistant Professor of Mechanics